

# Probing Ligand Protein Binding Equilibria with Fluorescence Fluctuation Spectroscopy

Yan Chen,\* Joachim D. Müller,\* Sergey Y. Tetin,<sup>†</sup> Joan D. Tyner,<sup>†</sup> and Enrico Gratton\*

\*Laboratory for Fluorescence Dynamics, University of Illinois at Urbana-Champaign, Urbana, Illinois 61801, and <sup>†</sup>Abbott Diagnostics Division, Abbott Laboratories, Abbott Park, Illinois 60064, USA

**ABSTRACT** We examine the binding of fluorescent ligands to proteins by analyzing the fluctuation amplitude  $g(0)$  of fluorescence fluctuation experiments. The normalized variance  $g(0)$  depends on the molecular brightness and the concentration of each species in the sample. Thus a single  $g(0)$  measurement is not sufficient to resolve individual species. Titration of the ligand with protein establishes the link between molecular brightness and concentration by fitting  $g(0)$  to a binding model and allows the separation of species. We first apply  $g(0)$  analysis to binary dye mixtures with brightness ratios of 2 and 4 to demonstrate the feasibility of this technique. Next we consider the influence of binding on the fluctuation amplitude  $g(0)$ . The dissociation coefficient, the molecular brightness ratio, and the stoichiometry of binding strongly influence the fluctuation amplitude. We show that proteins with a single binding site can be clearly differentiated from proteins with two independent binding sites. The binding of fluorescein-labeled digoxigenin to a high-affinity anti-digoxin antibody was studied experimentally. A global analysis of the fluctuation amplitude and the fluorescence intensity not only recovered the dissociation coefficient and the number of binding sites, but also revealed the molecular heterogeneity of the hapten-antibody complex. Two species were used to model the molecular heterogeneity. We confirmed the molecular heterogeneity independently by fluorescence lifetime experiments, which gave fractional populations and molecular brightness values that were virtually identical to those of the  $g(0)$  analysis. The identification and characterization of molecular heterogeneity have far-reaching consequences for many biomolecular systems. We point out the important role fluctuation experiments may have in this area of research.

## INTRODUCTION

There are few chemical systems that consist of a single species; these are useful, from an experimental point of view, as simple model systems. Biological systems typically contain more than one species, which interact to fulfill their biological function. The fast and unequivocal identification and functional characterization of different species of a biological system is a challenging and interesting problem.

Fluorescence correlation spectroscopy (FCS) has proved to be a powerful technique for characterizing multiple species in biological systems (Starchev et al., 1999; Widengren and Rigler, 1998; Haupts et al., 1998; Rauer et al., 1996). FCS exploits the fluorescence fluctuations originating from a small observation volume. The analysis of the temporal decay of the autocorrelation function,  $g(\tau)$ , provides rate coefficients that characterize the kinetic processes of the experimental system (Magde et al., 1972; Elson and Magde, 1974). Brownian motion causes molecules to diffuse through the observation volume. The autocorrelation function characterizes the average residence time of the molecules inside the observation volume. The size of the obser-

vation volume connects the residence time to the diffusion coefficient. If a mixture of species is present, and their hydrodynamic radius differs significantly, the autocorrelation function can be used to resolve multiple species (Wohland et al., 1999; Schuler et al., 1999; Van Craenenbroeck and Engelborghs, 1999; Klingler and Friedrich, 1997; Kinjo and Rigler, 1995). To resolve two species by their diffusion coefficient, a difference of  $\sim 2$  is needed, which corresponds to a molecular weight ratio of 8 (Meseth et al., 1999). For example, the autocorrelation function alone is not sufficient to distinguish proteins in their monomeric or dimeric form. Thus resolving multiple species based on their molecular weight alone imposes a severe limit on the practical use of FCS.

To overcome the limitation of the pure autocorrelation approach, two different analytical methods have been introduced to resolve multiple species. These techniques resolve multiple species based on a difference in their molecular brightness instead of their diffusion coefficient. Higher order autocorrelation analysis (Palmer and Thompson, 1987, 1989a, b) and higher order moments analysis (Qian and Elson, 1990a, Qian and Elson, 1990 b) determine the molecular brightness from the moments of the experimental data. The second approach was introduced recently by our group and is based on the statistics of the photon counting histogram (PCH) (Chen et al., 1999). This method resolves multiple species by analyzing the photon count distributions. Biological molecules with either one or two dye labels can be successfully resolved by a single measurement (Müller et al., 2000).

Received for publication 15 November 1999 and in final form 17 April 2000.

Address reprint requests to Dr. Enrico Gratton, Laboratory for Fluorescence Dynamics, University of Illinois at Urbana-Champaign, 184 Loomis Lab, 1110 W. Green St., Urbana, IL 61801. Tel.: 217-244-5620; Fax: 217-244-7187; E-mail: enrico@scs.uiuc.edu.

© 2000 by the Biophysical Society

0006-3495/00/08/1074/11 \$2.00

In this article we investigate ligand-protein equilibria. Specifically, we perform titration experiments to characterize the binding of a hapten to antibody and use the fluorescence fluctuation amplitude  $g(0)$  to analyze titration experiments. For a single species the  $g(0)$  value is inversely proportional to the number of molecules inside the observation volume. By monitoring the changes in the  $g(0)$  values, one can detect molecular dissociation or aggregation of fluorescent molecules (Berland et al., 1996). For more than one species, the direct relationship between the  $g(0)$  value and the number of molecules breaks down, and one has to take the fractional fluorescent intensity of the individual species into account. Thus when two species have identical or similar molecular weights but differ in their molecular brightness, the fluctuation amplitude contains useful information for the resolution of the species.

The direct calculation of the fluorescence fluctuation amplitude  $g(0)$  from the photon counts leads to an inflated value due to the shot-noise contribution. To arrive at the correct value of the fluctuation amplitude, the autocorrelation function is typically measured and fit to a model. The extrapolated time zero value of the fit provides  $g(0)$ . In this paper, we use moment analysis to determine  $g(0)$ , which was introduced by Qian and Elson (1990b). This analysis technique is based on shot-noise subtraction, which utilizes the relationship between intensity and photon count moments (Mandel, 1958; van Kampen, 1981). Thus  $g(0)$  is calculated directly from the photon counts, which is extremely fast and easy to perform. This technique requires no hardware correlators and no fitting procedures.

Binary dye mixtures are used to demonstrate the dependence of  $g(0)$  on the molecular brightness. Dyes are small molecules. The difference in their diffusion coefficients is insufficient for the resolution of multiple species. The molecular brightness difference of the dyes, however, affects the fluctuation amplitude significantly and reflects the composition of the binary mixture. We further consider ligand protein titration experiments from a theoretical point of view and determine the influence of the molecular brightness upon  $g(0)$ . The fit of the  $g(0)$  curve of a titration experiment provides both the binding constant and the number of independent binding sites of the system. We experimentally study the binding of fluorescein-labeled digoxigenin to a high-affinity monoclonal antibody. The simultaneous (global) fit of  $g(0)$  and the intensity curve not only recovers the binding coefficient  $K_D$  and the number of binding sites, but also identifies the heterogeneity of the complexed antibody. We confirmed this heterogeneity by an independent measurement of the fluorescence lifetime. Lifetime and fluctuation experiments probe molecular heterogeneity on widely different time scales, so that the limit on the interconversion rate between the heterogeneous populations can be inferred.

## MATERIALS AND METHODS

### Instrumentation

The instrumentation used for two-photon fluorescence fluctuation experiments is similar to that described by Chen et al. (1999). A mode-locked Ti:sapphire laser (Mira 900; Coherent, Palo Alto, CA) pumped by an intracavity doubled Nd:YVO<sub>4</sub> vanadate laser (Coherent) was used as the two-photon excitation source. The experiments were carried out with a Zeiss Axiovert 135 TV microscope (Thornwood, NY) with a 40× Fluor oil immersion objective (NA = 1.3). For all measurements, an excitation wavelength at 780 nm was used, and the average power at the sample ranged from 15 to 20 mW. Photon counts were detected with an APD (SPCM-AQ-161; EG&G). The output of the APD unit, which produces TTL pulses, was directly connected to a home-build data acquisition card (Eid et al., 2000). The photon counts were sampled at 20 kHz for dye measurements or at 80 kHz for the antibody binding study. The recorded and stored photon counts were later analyzed with programs written for PV-WAVE, version 6.10 (Visual Numerics, Inc.), and LFD Globals Unlimited software (Champaign, IL).

Fluorescence lifetime measurements were performed with a multifrequency cross-correlation phase fluorometer (Gratton et al., 1984). A 488-nm argon ion laser (Stabilite 2017; Spectra Physics) was used as the light source. Phase and modulation data were collected for 12 modulation frequencies in the range of 4–180 MHz. Fluorescence decay data were analyzed with Globals Unlimited software.

### Sample preparation

Rhodamine 110, 3-cyano-7-hydroxycoumarin, and fluorescein were purchased from Molecular Probes (Eugene, OR). All dyes were dissolved in 50 mM Tris[hydroxymethyl]amino-methane (Sigma, St. Louis, MO), and the pH was adjusted to 8.5 by adding HCl. Dye concentrations were determined by absorption measurements using the extinction coefficients provided by Molecular Probes.

Anti-digoxin monoclonal antibody (mAb) was obtained from a hybridoma cell line made by the fusion of spleen cells from RBf/DnJ mice immunized with digoxin-bovine serum albumin (Fitzgerald Industries, Concord, MA) and SP2/0 myeloma cells by a standard method (Goding, 1996). The cell line was cloned two times to ensure homogeneous cell population: once by limiting dilution and once by single-cell clone pick micromanipulation with Quixell (Stoelting, Wood Dale, IL). The mAb's isotype was determined to be mouse IgG1 ( $\kappa$ ) with Clonotyping System-HRP (Southern Biotechnology Associates, Birmingham, AL). The antibody was purified from tissue culture media on Poros Protein A (Perseptive Biosystems, Framingham, MA). The purity of the protein was verified by sodium dodecyl sulfate gel electrophoresis. The monoclonal character of the antibody was confirmed by isoelectric focusing (Pharmacia PhastSystem, pH gradient 3–10), revealing a pI of 6.55–7.35, with the typical microheterogeneity of a mouse monoclonal IgG.

Fluorescein-labeled digoxigenin (Abbott Laboratories, IL) was used in this study as the ligand. It has a molar extinction coefficient ( $\epsilon^M$ ) of 65,800 M<sup>-1</sup> cm<sup>-1</sup> at 494 nm and retains 0.8 of the fluorescein quantum efficiency. This tracer is 99% pure, as confirmed by analytical high-performance liquid chromatography.

The ligand was dissolved in 50 mM potassium phosphate buffer (pH 8.0) and kept at constant concentration of 1.33 nM during the experiment. Aliquots of antibody were added to 2 ml of ligand solution. The volume of the aliquot ranged from 1 to 8  $\mu$ l with varying antibody concentrations. The volume change due to the addition of antibody solution was less than 1% of the initial volume and thus is negligible for all practical calculations.

## DATA ANALYSIS

We use moment analysis with shot-noise subtraction to recover  $g(0)$  from experimental data (Qian and Elson, 1990a; 1991). This method calculates  $g(0)$  directly from the first and second moments of the photon counts but ignores the dynamic information of the autocorrelation function. A discussion regarding the signal statistics of moments appears in a paper by Kask et al. (1997).

### $g(0)$ analysis of a single species

In fluorescence fluctuation experiments, the  $g(0)$  values of a single fluorescent species, the time zero values of the autocorrelation function, depend on the average number of molecules inside the excitation volume (Thompson, 1991):

$$g(0) = \frac{\langle \Delta F^2 \rangle}{\langle F \rangle^2} = \frac{\gamma}{\bar{N}}, \quad (1)$$

where  $\gamma$  is a geometric factor and depends only on the shape of the excitation volume, and  $\bar{N}$  is the average number of molecules inside the observation volume.  $\langle \Delta F^2 \rangle$  is the variance and  $\langle F \rangle$  is the average intensity of the fluorescence intensity  $F$ . However, the experimental observable in a fluorescence fluctuation experiment is not the fluorescence intensity  $F$ , but the photon counts  $k$ . A direct calculation of  $g(0)$  based on the photon counts according to Eq. 1 leads to a vast overestimation of the  $g(0)$  value. There is a statistical relationship between the fluorescence intensity and the distribution of the photon counts (Mandel, 1958), which relates the factorial moments of the photon counts to the ordinary moments of the light intensity (van Kampen, 1981):

$$\langle F^m \rangle = \left\langle \frac{k!}{(k-m)!} \right\rangle = \langle k(k-1)(k-2) \cdots (k-m+1) \rangle. \quad (2)$$

Thus the first two moments of the fluorescence intensity are related to the moments of the photon counts,

$$\langle F \rangle = \langle k \rangle, \quad (3)$$

$$\langle F^2 \rangle = \langle k(k-1) \rangle = \langle k^2 \rangle - \langle k \rangle. \quad (4)$$

Equation 1 can now be rewritten in terms of the average and the variance of the photon counts,

$$g(0) = \frac{\langle \Delta F^2 \rangle}{\langle F \rangle^2} = \frac{\langle \Delta k^2 \rangle - \langle k \rangle}{\langle k \rangle^2}. \quad (5)$$

Our definition of the molecular brightness  $\varepsilon$  is similar to that of Chen et al. (1999):

$$\varepsilon = \frac{\langle k \rangle}{\bar{N}}, \quad (6)$$

where  $\varepsilon$  is expressed in counts per second per molecule (cpsm).

The main advantage of the direct calculation of  $g(0)$  from the first and second moments lies in its computational simplicity and model independence. The experimental accuracy of moment analysis was verified by performing photon counting histogram analysis, and virtually identical results were obtained with the two methods (Chen, 1999).

### $g(0)$ analysis of multiple species

The  $g(0)$  value for multiple species is the sum of all single species  $g(0)$  values weighted by the square of the fractional intensity (Thompson, 1991):

$$g(0) = \sum_{m=1}^M \left( \frac{\langle F_m \rangle}{\langle F_T \rangle} \right)^2 \cdot g_m(0) = \sum_{m=1}^M \left( \frac{\varepsilon_m \cdot \bar{N}_m}{\langle F_T \rangle} \right)^2 \cdot g_m(0), \quad (7)$$

where  $\langle F \rangle$  is the average fluorescence intensity in counts per second (cps), and  $M$  is the total number of species. The average fluorescence intensity of a mixture,  $\langle F_T \rangle$ , is given by  $\langle F_T \rangle = \sum_{m=1}^M \langle F_m \rangle$ . The intensity  $\langle F_m \rangle$  of the  $m$ th species is given, according to Eqs. 3 and 6, by

$$\langle F_m \rangle = \varepsilon_m \cdot \bar{N}_m. \quad (8)$$

For two species, A and B, the value of  $g(0)$  can be expressed in terms of the average number of molecules,  $\bar{N}_A$  and  $\bar{N}_B$ , and the molecular brightness,  $\varepsilon_A$  and  $\varepsilon_B$ :

$$g(0) = \gamma \frac{\varepsilon_A^2 \bar{N}_A + \varepsilon_B^2 \bar{N}_B}{(\varepsilon_A \bar{N}_A + \varepsilon_B \bar{N}_B)^2}. \quad (9)$$

If the brightnesses of the two species are identical, Eq. 9 reduces to the single species case, and  $g(0)$  again represents the total number of molecules  $\bar{N}$ . When the brightnesses of the two species differ,  $g(0)$  does not reflect the total number of molecules but depends on the brightness and the population of the individual species. Because  $g(0)$  represents only a single value, no discrimination between species is possible without additional information. However, if the two species are coupled by a binding equilibrium, then it is possible to establish the link between  $g(0)$  and the individual species by performing a titration experiment. The resulting  $g(0)$  values can be evaluated by fitting to a model. Photobleaching, triplet state, and other kinetic processes influence the  $g(0)$  value. If such processes are present the simple analysis based on Eq. 9 breaks down. The additional process effectively splits each population into subpopulations, which need to be explicitly considered in the analysis of the  $g(0)$  value. Under our experimental conditions no photobleaching or triplet state population was detected for any of the samples measured.

## RESULTS AND DISCUSSION

A titration experiment typically requires the systematic variation of the concentration of one compound, while keeping the concentrations of the other compound unchanged. It is necessary to change the concentration of one of the components by about several orders of magnitude to observe a complete titration curve. When one of the species is fluorescent, we titrate the fluorescent component by increasing the concentration of the nonfluorescent species. Therefore, the total number of fluorescent molecules is kept constant, but the fluorescence intensity changes according to the fractions of free and bound ligand if the binding affects fluorescence.

### Binary dye mixture

To mimic the condition of a ligand-protein titration experiment, we first study a binary dye mixture to demonstrate the principle of the experiment. The total number of dye molecules  $\bar{N}$  of the mixture is kept constant while the ratio of the two species is varied systematically. We use two different dye pairs: 1) 3-cyano-7-hydroxycoumarin with rhodamine 110 and 2) 3-cyano-7-hydroxycoumarin with fluorescein. Table 1 lists the molecular brightness,  $\varepsilon$ , and the average number of molecules,  $\bar{N}$ , of the three probes, as determined by moment analysis. Rhodamine 110 is the brightest fluorophore among the three dyes; for our experimental conditions, it is a factor of  $\sim 2$  brighter than fluorescein and a factor of 4 brighter than 3-cyano-7-hydroxycoumarin. The three dyes used for these experiments are relatively hydrophilic and do not absorb to the surfaces of the sample holder in the concentration range studied (Chen, 1999).

The results of the experiments are shown in Fig. 1. In the first experiment, we started with about three molecules of rhodamine 110 in the observation volume and gradually increased the fraction of 3-cyano-7-hydroxycoumarin to 100% (Fig. 1*A*). In the next experiment, we used the 3-cyano-7-hydroxycoumarin stock solution from the previous experiments and gradually increased the fraction of fluorescein to 100% (Fig. 1*B*). For each mixture, the  $g(0)$  values and the average photon counts  $\langle k \rangle$  were determined by moment analysis. Virtually identical results were obtained by photon counting histogram analysis (data not shown).

**TABLE 1** Properties of the fluorescent stock solutions

	3-Cyano-7-hydroxycoumarin	Fluorescein	Rhodamine 110
$\varepsilon$ (cpsm)	14,800	32,000	54,500
$\bar{N}$	2.61	3.26	2.99

All stock solutions have approximately the same concentration. The brightness ratio of 3-cyano-7-hydroxycoumarin to rhodamine 110 is 0.27, and that to fluorescein is 0.46.

Next we compare the experimentally determined fluctuation amplitudes and the average photon counts with theory. For two species A and B, the normalized population of species A is given by  $f = \bar{N}_A / (\bar{N}_A + \bar{N}_B)$ , and species B is given by  $1 - f$ . The average photon counts  $\langle k \rangle$  of the mixture are given by a linear combination of the photon counts  $\langle k_A \rangle$  and  $\langle k_B \rangle$ ,

$$\langle k \rangle = f \langle k_A \rangle + (1 - f) \langle k_B \rangle. \quad (10)$$

Thus, by using the experimentally obtained fluorescence intensity  $\langle k_A \rangle$  and  $\langle k_B \rangle$  and the molecular fraction of the individual species, we can calculate the theoretically expected fluorescence intensity,  $\langle k \rangle$ , from Eq. 10. A good match between the experimental intensity and the theoretical curve indicates a well-performed titration experiment (Fig. 1).

The theoretical expression of  $g(0)$  for a binary mixture is given by Eq. 9. The  $g(0)$  value of a mixture is a superposition of the  $g(0)$  values of the individual species weighted by the fractional intensity squared. Because the total number of fluorescent molecules stays constant during the titration experiment, Eq. 9 simplifies to

$$g(0) = \frac{\gamma}{\bar{N}} \cdot \left[ \frac{\varepsilon_A^2 f + \varepsilon_B^2 (1 - f)}{(\varepsilon_A f + \varepsilon_B (1 - f))^2} \right]. \quad (11)$$

If the brightnesses of the two species are identical, Eq. 11 reduces to the single-species case, and  $g(0)$  represents again the total number of molecules  $\bar{N}$ . Whenever the molecular brightnesses of the two species differ,  $g(0)$  does not reflect the total number of molecules, but depends on the brightness and the normalized population of the individual species.

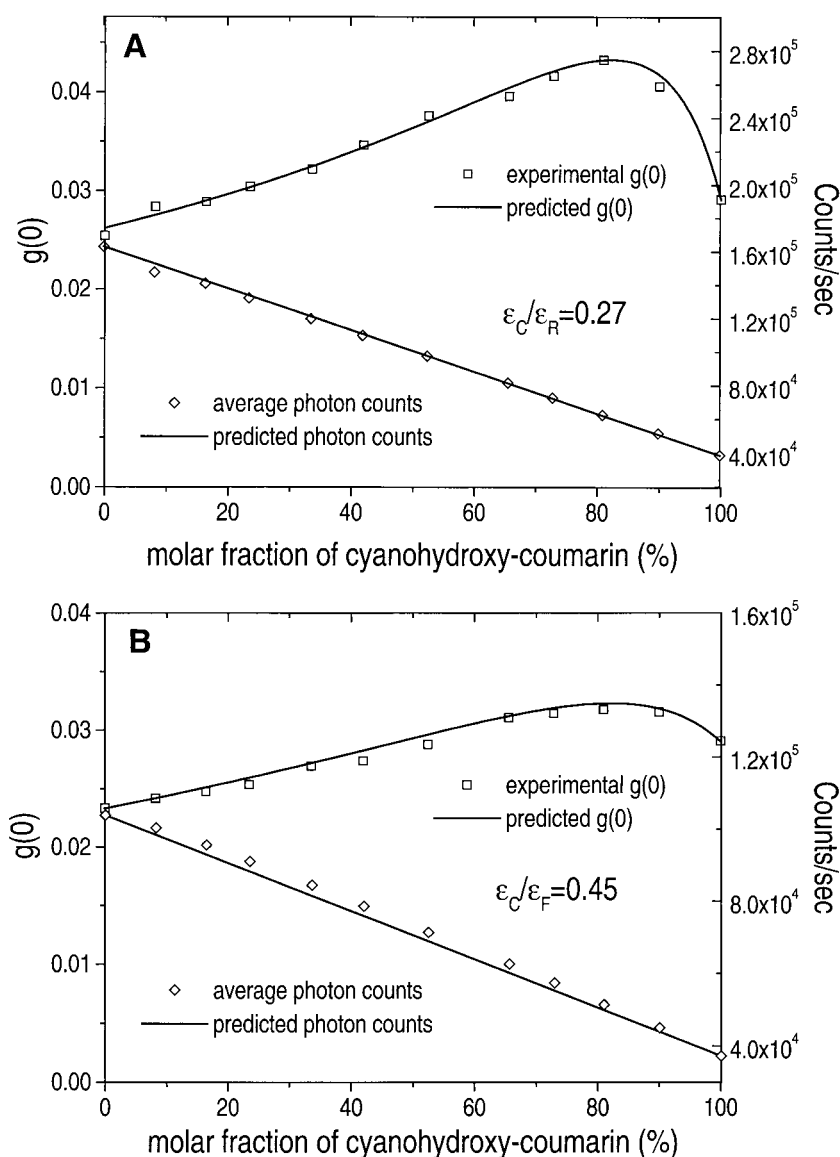
We used stock solutions of approximately the same dye concentration. By mixing the proper volumes of the stock solutions, the total number of molecules  $\bar{N}$  stays the same, and  $g(0)$  changes according to Eq. 11. In contrast to the average photon counts  $\langle k \rangle$ ,  $g(0)$  varies in a nonlinear fashion as a function of the fractional concentration of the species (see Fig. 1). The  $g(0)$  curve starts and ends with the same value, which simply reflects the fact that a single species of the same concentration is measured at the beginning and the end of the experiment. The  $g(0)$  value increases when the second component is added, approaches a maximum,  $g_{\max}(0)$ , and then decreases to its original value. The normalized fraction of species A,  $f_{\max}$ , where  $g_{\max}(0)$  is reached, can be determined from Eq. 11:

$$f_{\max} = \frac{1}{1 + \frac{\varepsilon_A}{\varepsilon_B}}. \quad (12)$$

The value of  $f_{\max}$  depends only on the brightness ratio of the dyes  $\varepsilon_A/\varepsilon_B$ . Thus an  $\varepsilon$  ratio of 0.27 for rhodamine 110 and 3-cyano-7-hydroxycoumarin predicts an  $f_{\max}$  of 0.79; a



FIGURE 1 The  $g(0)$  value and the fluorescence intensity of a binary dye mixture as a function of molar fraction. (A) 3-Cyano-7-hydroxycoumarin and rhodamine 110. (B) 3-Cyano-7-hydroxycoumarin and fluorescein. The total number of fluorescent molecules was kept approximately constant during the titration (Table 1). The theoretical  $g(0)$  and intensity values of the binary mixtures were calculated according to Eqs. 9 and 10 from the experimentally determined number of molecules  $\bar{N}$  and molecular brightness  $\varepsilon$  of the pure dyes (Table 1). The experimental  $g(0)$  ( $\square$ ) and average photon counts ( $\diamond$ ) are plotted together with their theoretically predicted curve (—). For cyano-7-hydroxycoumarin and fluorescein mixtures, a variation of 25% in the  $g(0)$  values is visible at the two end points of the titration curve. Differences in the stock concentration of both dyes are responsible for the difference in  $g(0)$ , as explained in the text.



brightness ratio of 0.45 for fluorescein and 3-cyano-7-hydroxycoumarin predicts an  $f_{\max}$  of 0.69. However, careful inspection of Fig. 1 reveals that the experimental  $f_{\max}$  deviates slightly from the theoretical value based on Eq. 12. We recovered an  $f_{\max}$  of 0.82 for the rhodamine 110 and 3-cyano-7-hydroxycoumarin pair, and 0.71 for the fluorescein and 3-cyano-7-hydroxycoumarin pair. This can be explained by the fact that the experimental stock concentrations of the different species, although close, are not exactly the same. Thus, to be precise, we have to use Eq. 9 instead of Eq. 11 to describe the experimental  $g(0)$  values.

By substituting Eq. 12 into Eq. 11, we obtain an analytic expression for  $g_{\max}(0)$ ,

$$g_{\max}(0) = g_{\min}(0) \cdot \left[ \frac{(1 + \varepsilon_A/\varepsilon_B)^2}{4(\varepsilon_A/\varepsilon_B)} \right], \quad (13)$$

where  $g_{\min}(0)$  is the  $g(0)$  value of the corresponding single-species case,  $g_{\min}(0) = \gamma\bar{N}$ . The ratio of  $g_{\max}(0)$  and  $g_{\min}(0)$  depends only on the brightness ratio of the dyes,  $\varepsilon_A/\varepsilon_B$ . Consequently, it is possible to calculate  $g_{\max}(0)$  from the brightness ratio of the two species, if the total number of fluorescent molecules is kept constant.

### Simulation of ligand-protein titration experiments

We just described the  $g(0)$  behavior of two noninteracting species with a fixed number of molecules. Now we transform the same concept to ligand protein titration experiments. Here we limit ourselves to the  $g(0)$  analysis of biopolymers with a fixed number of fluorescent ligands and explore the  $g(0)$  behavior. Our motivation is to gain infor-

mation about species from titration experiments, based only on differences in their molecular brightness values. We first discuss the binding of ligands to proteins with one binding site and then consider the binding of ligands to proteins with two independent binding sites.

The binding of a ligand to a single binding site of a biomolecule is, by definition, a two-species system. We can apply the formalism derived for the binary dye mixture directly to this system. The fractional population  $f$  of liganded biomolecules is given by a Henderson-Hasselbalch equation,  $f = [1/(1 + 10^{\log[L] - \log[K_D]})]$ , which is a consequence of the bimolecular reaction  $L + P \xrightleftharpoons{K_D} C$ , with a dissociation coefficient  $K_D$ . The fluorescent ligand  $L$  with a molecular brightness  $\varepsilon_L$  binds to the nonfluorescent protein  $P$  to form the complex  $C$  with a molecular brightness  $\varepsilon_C$ . We calculate  $f$  for a fixed ligand concentration as a function of the total protein concentration. Instead of using a linear concentration scale as in the case of the binary dye mixture, the titration of the binding sites is best displayed on a logarithmic concentration scale. Fig. 2 shows the fluctuation amplitude  $g(0)$  as a function of the total protein concentration for brightness ratios of 1, 4, 8,  $\frac{1}{4}$ , and  $\frac{1}{8}$ , assuming a dissociation coefficient  $K_D$  of 5 nM and a total ligand concentration of 5 nM. The solid line with filled circles in Fig. 2 represents a brightness ratio of 8, but for a  $K_D$  of 20 nM.

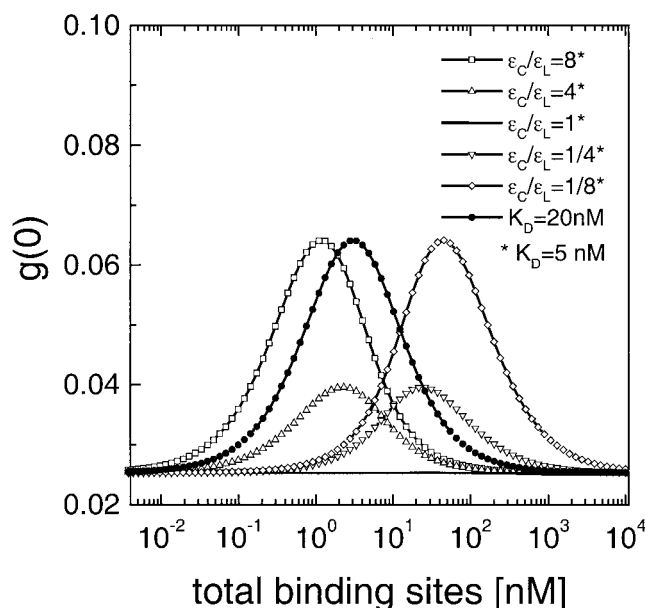


FIGURE 2 Simulation of  $g(0)$  titration curves for a single binding site. The ligand concentration is fixed at 5 nM. The  $g(0)$  values are plotted as a function of total binding site concentration. The peak position and peak height of  $g(0)$  depend strongly on the dissociation coefficient  $K_D$  and the brightness ratio  $\varepsilon_C/\varepsilon_L$  between the bound and free ligand. The brightness ratio of the two species is varied systematically, while keeping the dissociation coefficient ( $K_D = 5$  nM) constant (open symbols). The solid symbols represent the titration curve for a  $K_D$  of 20 nM and a brightness ratio of 8.

The total number of fluorescent molecules does not change for a single binding site reaction. For equal brightness values of bound and free ligand,  $g(0)$  is inversely proportional to the total number of fluorescent molecules and independent of the protein concentration. For different brightness values of the free and bound ligand,  $g_{\max}(0)$  can be determined by Eq. 13 as long as  $\varepsilon_C$  and  $\varepsilon_L$  are known. In fact, any discrepancy between the predicted and measured  $g_{\max}(0)$  indicates that the binding cannot be described by the simple binding model described so far.

Next we examine the binding of a ligand to two independent binding sites. The binding of hapten to immunoglobulin G (IgG) antibodies is an example of such a reaction. There are now three fluorescent species to consider: the free ligand and antibody with either one or two bound ligands. The calculation of the concentration of the free ligand,  $L$ , the singly liganded protein,  $PL$ , and the doubly liganded species,  $PL_2$ , is straightforward (Cantor and Schimmel, 1980; Winzor and Sawyer, 1995). The binding of ligands to protein with a single site or two independent binding sites leads to exactly the same intensity dependence as a function of protein concentration. However, this is not the case for the fluctuation amplitude  $g(0)$ . The molecular brightness of the doubly liganded species  $\varepsilon_{2C}$  is twice the value of the singly liganded species  $\varepsilon_C$ . When an antibody with two ligands leaves the excitation volume, the intensity change is equivalent to the simultaneous loss of two singly liganded antibodies. Thus the intensity fluctuations associated with the doubly liganded antibody are stronger than those associated with the singly liganded one.

Three species with molecular brightness values of  $\varepsilon_L$ ,  $\varepsilon_C$ , and  $\varepsilon_{2C}$  contribute to the fluctuation amplitude. The calculation of the fluctuation amplitude  $g(0)$  requires the use of Eq. 7 together with the proper binding model, which connects the populations of the different species. The calculations were carried out with parameters identical to those for the single-species case. The results of the simulations are shown in Fig. 3 A. The differences of the  $g(0)$  curves when compared to Fig. 2 reflect the influence of the second binding site. Even if the binding of the ligand does not lead to a change in the fluorescence intensity ( $\varepsilon_C = \varepsilon_L$ ), contrary to the single binding site case,  $g(0)$  is not constant. A small  $g(0)$  peak appears, which is caused by the additional fluctuations of the doubly liganded antibody.

The two-ligand bound species exists only at specific protein concentrations. When the protein concentration is far below its  $K_D$ , most ligands are free, and the probability that the antibody carries two ligands is very small. When the protein concentration is much larger than the total ligand concentration, proteins start to compete for the free ligand, which results in a negligible amount of protein with two ligands. To better illustrate the influence of the doubly liganded species, the fractional populations of the free ligand and the antibody with one or two ligands are plotted as a function of the total concentration of antibody binding

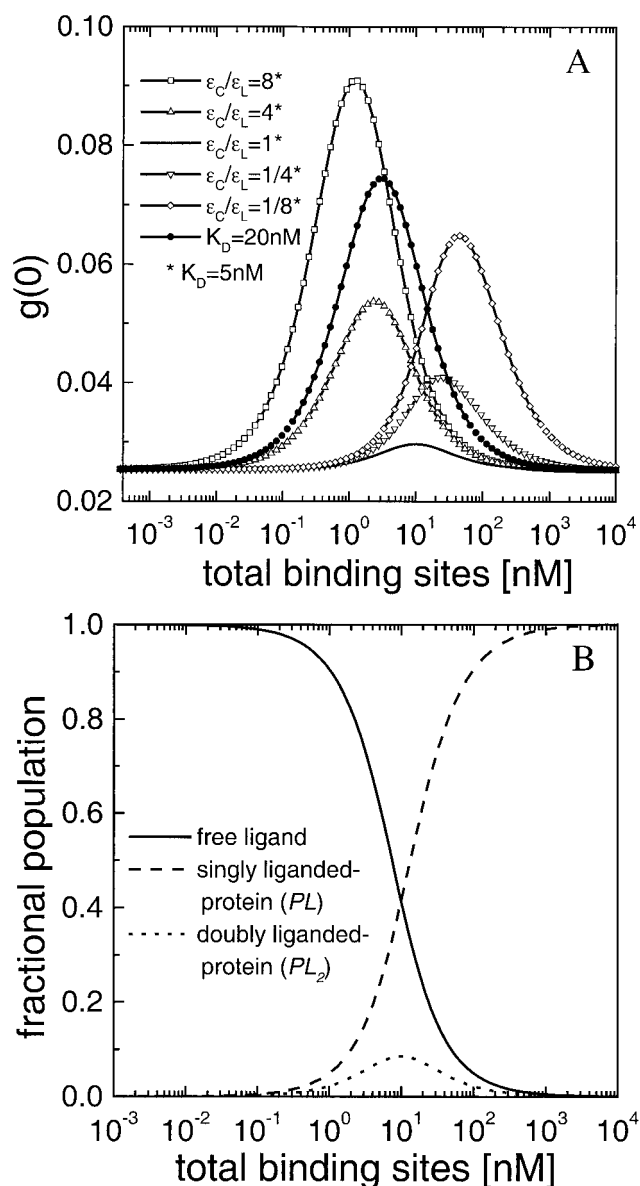


FIGURE 3 (A) Simulation of  $g(0)$  titration curves for two binding sites. The symbols and the simulation parameters are identical to the ones used for Fig. 2, with the exception that two independent binding sites are considered. The presence of a third species, the doubly liganded species, which is twice as bright as the singly liganded species, leads to stronger intensity fluctuations. (B) The fractional populations of a titration experiment for a protein with two equivalent binding sites. The fractional population of the free ligand and protein with one or two bound ligands is plotted as a function of total binding site concentration. The  $K_D$  and the total ligand concentration used for this calculation are 5 nM. The fractions of free ligand and protein with a single ligand vary from 1 to 0. The curve of the fraction of the doubly liganded species varies in a bell-shaped fashion.

sites for a  $K_D$  of 5 nM and a total ligand concentration of 5 nM (Fig. 3 B). Under these conditions, the maximum of the doubly liganded species,  $PL_2$ , accounts for less than 10% of the total population of fluorescent molecules. However, the

$PL_2$  species has a strong influence on the observed fluctuation amplitude, because  $PL_2$  is twice as bright as  $PL$ . This is especially true when the molecular brightness  $\varepsilon_C$  is enhanced upon binding. For example, a brightness ratio of  $\varepsilon_C/\varepsilon_L = 8$  yields a  $g_{\max}(0)$  that is 1.5 times larger than  $g_{\max}(0)$  for the reciprocal brightness ratio of  $\varepsilon_C/\varepsilon_L = \frac{1}{8}$ . Thus, in contrast to the titration of a single binding site, the symmetry of reciprocal brightness ratios is broken because of the contribution of the doubly liganded species.

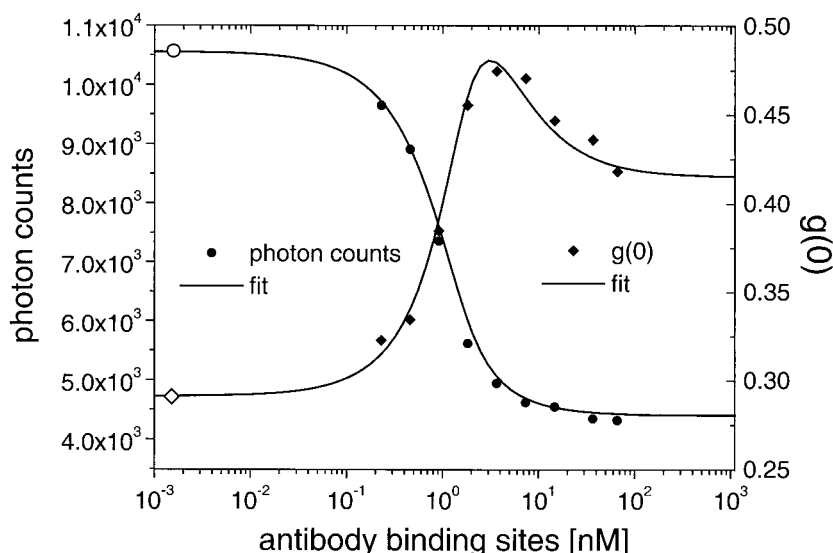
For a single binding site, the  $g_{\max}(0)$  value is independent of the dissociation coefficient  $K_D$  and only depends on the brightness ratio of the two species. But for two binding sites, the  $g_{\max}(0)$  value varies as a function of the dissociation coefficient  $K_D$ , even if the brightness ratio  $\varepsilon_C/\varepsilon_L$  stays constant, as illustrated in Fig. 3 A. This again is due to presence of the population of the doubly liganded species. An increase in the dissociation coefficient  $K_D$  requires a higher concentration of protein to bind an equivalent fraction of ligand. Hence, more protein molecules compete for the same amount of ligands. The population of the  $PL_2$  species gradually decreases, while  $g_{\max}(0)$  reaches the asymptotic value of the single species case in the limit of large  $K_D$  values.

### Anti-digoxin antibody binding study

The result of the titration of fluorescently labeled digoxigenin with anti-digoxin antibody is shown in Fig. 4. The  $g(0)$  values are directly determined from the raw data by moment analysis. The error of each point was determined by repeating the experiments several times. We recovered an experimental uncertainty of 3%. Both the fluorescence intensity and  $g(0)$  are displayed as a function of the total concentration of antibody binding sites. The fluorescence of the ligand is quenched upon binding to the antibody. A large excess of antibody over hapten leads to the formation of a singly liganded complex ( $PL$ ). Thus the limiting  $g(0)$  value at high protein concentration and the  $g(0)$  value of the free ligand alone should be identical, regardless of the brightness difference between the two species. However, experimentally we observe that the  $g(0)$  values at the beginning and end of the titration are not identical (see Fig. 4). The ratio of the  $g(0)$  value between the free and singly bound ligand is  $\sim 1.4$ .

This discrepancy of the experimentally observed  $g(0)$  from the theoretically predicted value indicates that, contrary to our assumption, either the total number of fluorescent molecules changed or more than one species contributes to the  $g(0)$  value of the singly bound species. The  $g(0)$  value of the singly bound antibody ( $PL$ ) is higher than the initial free ligand value. This could be explained by a loss of molecules due to adsorption to the walls of the sample container. However, performing the experiment with a fresh sample container or the same container for each titration step gave identical  $g(0)$  values. Thus adsorption of mole-

FIGURE 4 Titration experiment of digoxigenin and anti-digoxin antibody. The total ligand concentration is 1.33 nM. By simultaneously fitting intensity and  $g(0)$ , we recovered a dissociation coefficient of  $K_D = 300$  pM. Two molecular species were recovered by the fit for the antibody complex. The molecular fractions and brightness values are given in Table 2. The excitation volume of the measurement was  $\sim 0.32$  fl. The experimental  $g(0)$  ( $\blacklozenge$ ) and average photon counts ( $\bullet$ ) are plotted together with their theoretical curve (—). The  $g(0)$  value ( $\diamond$ ) and average photon counts ( $\circ$ ) of the free ligand are also drawn on the graph for comparison.



cules to surfaces cannot explain the change in the  $g(0)$  value. We also checked the autocorrelation functions of free and bound ligands and observed no triplet state reaction or any other kinetic processes that would contribute to the value of  $g(0)$  (data not shown).

Alternatively, the difference in the  $g(0)$  values of the free ligand and the singly liganded antibody could be explained by the presence of multiple species of the antibody complex. In fact, once we assumed that the singly liganded species consists of two component, we were able to fit  $g(0)$  and the intensity titration curves simultaneously with a dissociation coefficient  $K_D$  of 300 pM (Fig. 4). The brightness ratio of the two components (denoted as  $C_1$  and  $C_2$ ) recovered by the fit is  $\sim 4$  (Table 2). The molar fraction of the bright species  $C_1$  is 45%, while that of the dim species  $C_2$  is 55%. The coexistence of two fluorescent components of the bound antibody together with two independent binding sites requires the consideration of five fluorescent species, taking all possible permutations into account:  $C_1$ ,  $C_2$ ,  $C_1C_2$ ,  $C_1C_1$ , and  $C_2C_2$ . Together with the free ligand, this accounts for

**TABLE 2** Properties of the free and bound ligand as determined by fluorescence lifetime and fluorescence fluctuation experiments

	Lifetime (ns)	Relative population	Molecular brightness (cpsm)	Relative population
Digoxigenin	4.01	100%	40500	100%
Liganded digoxigenin ( $C_1$ )	4.01	48%	29000	45%
Liganded digoxigenin ( $C_2$ )	1.03	52%	6900	55%

The fluorescence lifetimes and their relative populations are measured for free and bound ligand. The molecular brightness and relative population of the free and bound ligand are determined from a titration experiment using fluorescence fluctuation spectroscopy.

the existence of six molecular species. But only three species, the free ligand,  $C_1$ , and  $C_2$ , are independent and are determined by the global fit of the intensity and fluctuation amplitude data. Based on the molecular fractions of  $C_1$  and  $C_2$  and their molecular brightness  $\epsilon_{C_1}$  and  $\epsilon_{C_2}$ , the doubly liganded species consists of three species,  $C_1C_1$ ,  $C_2C_2$ , and  $C_1C_2$ , with relative populations of 20%, 30%, and 50% and molecular brightness values of 58,000, 13,800, and 35,900 cpsm, respectively. When the antibody concentration is much less than the dissociation coefficient  $K_D$ , the free ligand is the dominant species, and there is almost no detectable doubly liganded antibody. When the antibody concentration approaches the  $K_D$  value, the amount of the doubly liganded species increases steadily and accounts for almost half of the bound population. However, the majority of antibody complexed with two ligands consists of  $C_1C_2$ , which has almost the same brightness as the free ligand, so that the brightness contrast is not very pronounced. Nevertheless, it is possible to detect an increase in  $g(0)$  as a function of the antibody concentration. When the antibody concentration exceeds the total ligand concentration, the antibody molecules start to compete for ligand, which results in the disappearance of the doubly liganded species at high antibody concentrations. However, because the brightness difference between  $C_1$  and  $C_2$  is more than a factor of 4,  $g(0)$  does not approach the value of the free ligand, but is increased by a factor of 1.4.

### Fluorescence lifetime study

The result of the titration experiment points to the molecular heterogeneity of the antibody complex. We do not know the origin of the two components,  $C_1$  and  $C_2$ , but we can distinguish them by their molecular brightness values. The



difference in the molecular brightness indicates two different conformations of the bound antibody complex, with different interactions between fluorophore and antibody. These differences in the molecular interactions lead to different amounts of dynamic quenching. However, dynamic quenching connects molecular brightness and fluorescence lifetime. A reduction of the fluorescence lifetime of a dye due to dynamic quenching leads to an equal decrease in the molecular brightness (Birks, 1970; Lakowicz, 1983). Therefore, we performed fluorescence lifetime experiments in the frequency domain to test this idea (Table 2).

For the fluorescein-labeled digoxigenin, we obtained a single lifetime of 4.01 ns. However, two lifetime components were recovered for digoxigenin-bound antibody. We label both components with  $C_1$  and  $C_2$ , analogously to the fluctuation experiments. The first component,  $C_1$ , has a lifetime of 4.01 ns, with a molecular fraction of 48%.  $C_2$  has a significantly shorter lifetime of 1.03 ns, with a molecular fraction of 52%. The ratio of the two lifetimes is almost equal to the brightness ratio obtained from the  $g(0)$  measurements, which is consistent with dynamic quenching. Moreover, the two techniques recover virtual identical populations for  $C_1$  and  $C_2$  (Table 2).

Because two independent experimental techniques recover the same properties for the two components,  $C_1$  and  $C_2$ , we infer that the two measurements probe the same conformational states of the bound complex. However, the two techniques probe heterogeneity on two widely different time scales. Fluorescence lifetime measurements probe the protein during the lifetime of the fluorophore, which is on the nanosecond time scale. Fluorescence fluctuation experiments probe the hapten-antibody complex on the time scale of the sampling clock, which in our experiments was close to 10  $\mu$ s. Thus the experiments show the persistence of the two states  $C_1$  and  $C_2$  from nanoseconds to at least 10  $\mu$ s.

### Fluctuation amplitude analysis of binding equilibria

Two species with exactly the same brightness are indistinguishable by  $g(0)$  analysis. In this case, the autocorrelation function can be used to separate two species, if their diffusion coefficients differ sufficiently. The molecular weight difference of the species has to be at least a factor of 5–8 to separate species by their diffusion coefficient alone (Meseth et al., 1999). This approach has been used to characterize the binding of small ligands to macromolecules (Rauer et al., 1996).

Fluorescently labeled biological samples, however, often exhibit pronounced differences in their molecular brightness but not in their molecular mass. A protein dimer, formed by the association of two monomers, is twice as bright as the monomer if no quenching occurs upon binding. The conformation of protein substates or the structural heterogeneity of DNA molecules can influence the spectroscopic prop-

erties of fluorescent dyes, which are often sensitive to the local environment of the macromolecules.

The fluctuation amplitude  $g(0)$  represents only a single value and therefore is not sufficient to discriminate between species without further knowledge. However, a thermodynamic binding model of ligand protein binding provides enough information to establish the link between  $g(0)$  and the individual fluorescent species. The  $g(0)$  values, the brightness  $\varepsilon$ , and the average number of molecules  $\bar{N}$  are not independent of one another, but are related to the experimentally determined fluorescence intensity (Eqs. 3, 6, and 8). For a mixture of two species, A and B, the average intensity is given by  $\langle k \rangle = \varepsilon_A \bar{N}_A + \varepsilon_B \bar{N}_B$ . Therefore, we fit the average photon counts  $\langle k \rangle$  and the fluctuation amplitude  $g(0)$  simultaneously to a binding model. Typically, it is possible to determine the molecular brightness  $\varepsilon$  and the average number of molecules  $\bar{N}$  of the fluorescent ligand directly; this information can then be used as a constraint in the fitting procedure. The global analysis of the  $g(0)$  values and fluorescence intensity,  $\langle k \rangle$ , allows us not only to recover the binding constant and the number of independent binding sites, but also to detect molecular heterogeneity and to resolve it by fitting to the experimental data.

A single-binding-site model will not be able to describe the  $g(0)$  titration curve of a protein with two binding sites, because the additional intensity fluctuation of the doubly liganded species increases  $g(0)$ . Likewise, a two-binding-site model will overestimate the  $g(0)$  values of a titration experiment with a single binding site. By analyzing the  $g(0)$  titration curve in conjunction with the intensity data, we can recover the number of binding sites from the fluorescence fluctuation experiment. The number of binding sites cannot be obtained from the intensity data alone.

The molecular weight difference between the antibody and the ligand is more than a factor of 100. Thus the amount of free and bound ligand can be resolved from the autocorrelation function by the difference in their diffusion coefficients. Autocorrelation analysis would give us an additional advantage in resolving molecular species. However, the diffusion coefficients of the singly and doubly liganded protein are virtually identical and cannot be used to resolve the two species by the autocorrelation function. To interpret the experimentally recovered amplitude of the free and bound ligand from the autocorrelation function, exactly the same type of analysis as presented in this paper has to be performed to connect the amplitude to the fractional population of each species. Here we focus on the analysis of binding equilibria by the fluctuation amplitude alone, which is sufficient to resolve species as long as the molecular brightness changes upon binding.

### Heterogeneity of biomolecules

Biological macromolecules are without doubt complicated systems. Here we choose fluorescence lifetime and fluores-

cence fluctuation techniques to characterize the binding of fluorescein-labeled digoxigenin (digoxigenin-FL) to an anti-digoxin antibody. The existence of two lifetime components for the bound complex compared to the single lifetime of the free ligand indicates that there are two states  $C_1$  and  $C_2$  for the bound complex. Therefore, we conclude that two distinct states exist on the time scale of a few nanoseconds. Biological molecules often display multiple lifetime components or a distribution of lifetimes. It is important for us that the fluorescence fluctuation data indicate the existence of two states with almost exactly the same properties as recovered from the lifetime measurement. The molecular brightnesses recovered by the two measurements are almost equal, and the brightness ratio is consistent with the lifetime ratio of the two states. Thus it is most likely that the two measurements characterize the same states, which means that the two states have not interchanged on the sampling time scale of the fluorescence fluctuation experiment. If the two states would interconvert faster than the sampling time, then we would observe only the averaged property of the two states. The sampling time of the fluorescence fluctuation measurement is  $12.5 \mu\text{s}$ , which is several orders of magnitude longer than the fluorescence lifetime. The parameters obtained from the lifetime measurements are only meaningful for fluorescence fluctuation measurements if the states involved preserve their properties from the nanosecond time scale to  $\sim 10 \mu\text{s}$ .

Actually, if the two states interconvert during the time it takes to diffuse through the observation volume of the microscope, the autocorrelation function captures this kinetic process (Bonnet et al., 1998; Haupts et al., 1998). We analyzed the autocorrelation function of the bound antibody. A simple diffusion model describes the experimental correlation function, and no exchange kinetic is visible (data not shown). Thus we conclude that the two states do not interconvert to at least a millisecond, which is the diffusion time of the protein complex in the laser illumination volume.

The specific origin of the heterogeneity of the protein sample is unknown to us. However, proteins in general exist in a variety of conformational substates, which are responsible for their heterogeneity. The interconversion time of conformational substates ranges from nanoseconds to almost infinity and depends on many external parameters, such as temperature. Fluorescence techniques have been used to probe conformational substates (Alcala et al., 1987). However, the interconversion between conformational substates at room temperature on time scales longer than microseconds is hard to characterize with existing techniques. Single-molecule spectroscopy is one of the few techniques that allows the study of conformational substates on the millisecond and longer time scales (Lu et al., 1998; Moerner and Orrit, 1999). Fluorescence fluctuation spectroscopy offers another potentially powerful method for probing the heterogeneity of proteins.

Another important consequence of our results concerns the interpretation of the fluctuation amplitude  $g(0)$  in fluorescence correlation experiments. The fluctuation amplitude only characterizes the average number of molecules in the excitation volume, if a single species is measured. Tagging of fluorescent dyes to biomolecules can result in rather complex interactions between the dye and the biomolecule (Vamosi et al., 1996). In such a case, it is likely that several molecular species with different molecular brightness values contribute to the fluctuation amplitude. An averaged molecular species will be measured only if the different states interconvert on a time scale faster than the sampling time chosen for the fluctuation experiment. In all other cases, the fluctuation amplitude  $g(0)$  is not necessarily a measure of the absolute concentration of the biomolecule of interest.

Here we exploit the fluctuation amplitude and link it to an equilibrium-binding model, which allowed us to detect and characterize the molecular heterogeneity of an antibody complex. The molecular heterogeneity of fluorescently tagged biomolecules, on the other hand, cannot be resolved by a single measurement of  $g(0)$  alone, but requires a complete titration experiment. However, the analysis of the fluctuation data by the photon counting histogram (PCH) can overcome the limitation of the fluctuation amplitude approach, because it allows the resolution of molecular heterogeneity from a single measurement (Müller et al., 2000).

## CONCLUSIONS

We demonstrated that the fluctuation amplitude  $g(0)$  is valuable for the study of binding equilibria of biomolecules. The nonlinear influence of the molecular brightness on the fluctuation amplitude provides information that is not accessible from the fluorescence intensity alone. For example, the response of the fluctuation amplitude  $g(0)$  to a ligand binding study of a single binding site is rather different from one involving two binding sites. The binding of digoxigenin to anti-digoxin antibody was analyzed by globally fitting the fluctuation amplitude  $g(0)$  and the average photon counts  $\langle k \rangle$ , which specified the dissociation coefficient and the number of binding sites. Furthermore, we identified the molecular heterogeneity of the hapten-antibody complex and resolved the relative populations of two states and their corresponding molecular brightness values. Fluorescence lifetime measurements of the liganded antibody also revealed two states with relative populations and molecular brightness values that were virtually identical to that obtained by fluctuation amplitude analysis. This result indicates that the two techniques probe the same states, which do not interconvert on a time scale from nanoseconds to at least milliseconds. Thus fluorescence fluctuation experiments could be valuable for the characterization of both the dynamics and the molecular heterogeneity of biomolecules.

## REFERENCES

- Alcala, J. R., E. Gratton, and F. G. Prendergast. 1987. Interpretation of fluorescence decays in proteins using continuous lifetime distributions. *Biophys. J.* 51:925–936.
- Berland, K. M., P. T. C. So, Y. Chen, W. W. Mantulin, and E. Gratton. 1996. Scanning two-photon fluctuation correlation spectroscopy: particle counting measurements for detection of molecular aggregation. *Biophys. J.* 71:410–420.
- Birks, J. B. 1970. *Photophysics of Aromatic Molecules*. Wiley Interscience, London and New York.
- Bonnet, G., O. Krichavsky, and A. Libchaber. 1998. Kinetics of conformational fluctuations in DNA hairpin loops. *Proc. Natl. Acad. Sci. USA*. 95:8602–8606.
- Cantor, C. R., and P. R. Schimmel. 1980. *Biophysical Chemistry*. W. H. Freeman and Company, New York.
- Chen, Y. 1999. *Analysis and Applications of Fluorescence Fluctuation Spectroscopy*. University of Illinois at Urbana-Champaign, Urbana, IL (available at <http://web.physics.uiuc.edu/Research/Fluorescence/index.html>).
- Chen, Y., J. D. Muller, P. T. So, and E. Gratton. 1999. The photon counting histogram in fluorescence fluctuation spectroscopy. *Biophys. J.* 77: 553–567.
- Eid, J. S., J. D. Müller, and E. Gratton. 2000. Data acquisition card for fluctuation correlation spectroscopy allowing full access to the detected photon sequence. *Rev. Sci. Instrum.* 71:361–368.
- Elson, E. L., and D. Magde. 1974. Fluorescence correlation spectroscopy. I. Conceptual basis and theory. *Biopolymers*. 13:1–27.
- Goding, J. W. 1996. *Monoclonal Antibodies: Principles and Practice*. Academic Press, London.
- Gratton, E., D. M. Jameson, and R. D. Hall. 1984. Multifrequency phase and modulation fluorometry. *Annu. Rev. Biophys. Bioeng.* 13:105–124.
- Haupts, U., S. Maiti, P. Schwille, and W. W. Webb. 1998. Dynamics of fluorescence fluctuations in green fluorescent protein observed by fluorescence correlation spectroscopy. *Proc. Natl. Acad. Sci. USA*. 95: 13573–13578.
- Kask, P., R. Gunther, and P. Axhausen. 1997. Statistical accuracy in fluorescence fluctuation experiments. *Eur. Biophys. J.* 25:163–169.
- Kinjo, M., and R. Rigler. 1995. Ultrasensitive hybridization analysis using fluorescence correlation spectroscopy. *Nucleic Acids Res.* 23: 1795–1799.
- Klingler, J., and T. Friedrich. 1997. Site-specific interaction of thrombin and inhibitors observed by fluorescence correlation spectroscopy. *Biophys. J.* 73:2195–2200.
- Lakowicz, J. R. 1983. *Principles of Fluorescence Spectroscopy*. Plenum Press, New York and London.
- Lu, H. P., L. Xun, and X. S. Xie. 1998. Single-molecule enzymatic dynamics. *Science*. 282:1877–1882 (erratum: 283:35).
- Magde, D., E. Elson, and W. W. Webb. 1972. Thermodynamic fluctuations in a reacting system: measurement by fluorescence correlation spectroscopy. *Phys. Rev. Lett.* 29:705–708.
- Mandel, L. 1958. Fluctuations of photon beams and their correlations. *Proc. Phys. Soc.* 72:1037–1048.
- Meseth, U., T. Wohland, R. Rigler, and H. Vogel. 1999. Resolution of fluorescence correlation measurements. *Biophys. J.* 76:1619–1631.
- Moerner, W. E., and M. Orrit. 1999. Illuminating single molecules in condensed matter. *Science*. 283:1670–1676.
- Müller, J. D., Y. Chen, and E. Gratton. 2000. Resolving heterogeneity on the single molecular level with the photon counting histogram. *Biophys. J.* 78:474–486.
- Palmer, A. G. d., and N. L. Thompson. 1987. Molecular aggregation characterized by high order autocorrelation in fluorescence correlation spectroscopy. *Biophys. J.* 52:257–270.
- Palmer, A. G., III, and N. L. Thompson. 1989a. Intensity dependence of high-order autocorrelation functions in fluorescence correlation spectroscopy. *Rev. Sci. Instrum.* 60:624–633.
- Palmer, A. G. d., and N. L. Thompson. 1989b. High-order fluorescence fluctuation analysis of model protein clusters. *Proc. Natl. Acad. Sci. USA*. 86:6148–6152.
- Qian, H., and E. L. Elson. 1990a. Distribution of molecular aggregation by analysis of fluctuation moments. *Proc. Natl. Acad. Sci. USA*. 87: 5479–5483.
- Qian, H., and E. L. Elson. 1990b. On the analysis of high order moments of fluorescence fluctuations. *Biophys. J.* 57:375–380.
- Qian, H., and E. L. Elson. 1991. Analysis of confocal laser-microscope optics for 3-D fluorescence correlation spectroscopy. *Appl. Opt.* 30: 1185–1195.
- Rauer, B., E. Neumann, J. Widengren, and R. Rigler. 1996. Fluorescence correlation spectrometry of the interaction kinetics of tetramethylrhodamin alpha-bungarotoxin with *Torpedo californica* acetylcholine receptor. *Biophys. Chem.* 58:3–12.
- Schuler, J., J. Frank, U. Trier, M. Schafer-Korting, and W. Saenger. 1999. Interaction kinetics of tetramethylrhodamine transferrin with human transferrin receptor studied by fluorescence correlation spectroscopy. *Biochemistry*. 38:8402–8408.
- Starichev, K., J. Buffle, and P. r. E. 1999. Applications of fluorescence correlation spectroscopy: polydispersity measurements. *J. Colloid Interface Sci.* 213:479–487.
- Thompson, N. L. 1991. Fluorescence correlation spectroscopy. In *Topics in Fluorescence Spectroscopy*. J. R. Lakowicz, editor. Plenum, New York. 337–378.
- Vamosi, G., C. Gohlke, and R. M. Clegg. 1996. Fluorescence characteristics of 5-carboxytetramethylrhodamine linked covalently to the 5' end of oligonucleotides: multiple conformers of single-stranded and double-stranded dye-DNA complexes. *Biophys. J.* 71:972–994.
- Van Craenenbroeck, E., and Y. Engelborghs. 1999. Quantitative characterization of the binding of fluorescently labeled colchicine to tubulin in vitro using fluorescence correlation spectroscopy. *Biochemistry*. 38: 5082–5088.
- van Kampen, N. G. 1981. *Stochastic Processes in Physics and Chemistry*. Elsevier Science Publishing Company, New York.
- Widengren, J., and R. Rigler. 1998. Fluorescence correlation spectroscopy as a tool to investigate chemical reactions in solutions and on cell surfaces. *Cell Mol. Biol. (Noisy-le-grand)*. 44:857–879.
- Winzor, D. J., and W. H. Sawyer. 1995. *Quantitative Characterization of Ligand Binding*. Wiley-Liss, New York.
- Wohland, T., K. Friedrich, R. Hovius, and H. Vogel. 1999. Study of ligand-receptor interactions by fluorescence correlation spectroscopy with different fluorophores: evidence that the homopentameric 5-hydroxytryptamine type 3As receptor binds only one ligand. *Biochemistry*. 38:8671–8681.